SINERGI Vol. 26, No. 3, October 2022: 343-354
http://publikasi.mercubuana.ac.id/index.php/sinergi
http://doi.org/10.22441/sinergi.2022.3.010

Taguchi-based design of experiments to optimize the parameters of Hydrogen-Hydrogen-Oxygen based welding

Desi Fajarwati[1*], Deni Shidqi Khaerudini[1,2]
[1]Department of Mechanical Engineering, Faculty of Engineering, Universitas Mercu Buana, Indonesia
[2]Research Center for Physics, BRIN, Indonesia

Abstract
This study discusses the design of a hydrogen-hydrogen-oxygen (HHO) based welding tool, which uses the concept of water electrolysis through a dry cell generator. To determine the optimal design of the HHO dry cell generator, a design experiment was carried out using the Taguchi method by taking into account several parameters, namely the configuration of the electrode plate, the duty cycle Pulse Width Modulation (PWM), the type of catalyst, the electrolyte concentration, and the thickness of the gasket of the electrode plate. Each parameter is varied in 4 levels so that 16 kinds of experiments are obtained with an orthogonal array. In addition, the Combustion temperature data was collected after determining the optimal design. The experimental results show that this HHO-based welding tool is able to produce an average temperature reach of 1063.85 °C.

Keywords:
Dry cell;
HHO;
Taguchi;
Welding;

Article History:
Received: January 19, 2022
Revised: February 23, 2022
Accepted: March 11, 2022
Published: October 6, 2022

Corresponding Author:
Desi Fajarwati,
Department of Mechanical Engineering, Faculty of Engineering, Universitas Mercu Buana, Indonesia,
Email: desifajarw@gmail.com

INTRODUCTION

For thousands of years, methods for joining metals have been known, but some welding principles only emerged in the late 19th century. The method is to safely combine and store gases such as oxygen and acetylene to produce a flame with sufficient heat. The gas used for welding, oxyacetylene, was first discovered in France in the late 19th century by Edmund Fouche and Charles Picard [1]. The main characteristics of acetylene compared to other gases are shown in Table 1. Acetylene contains 92.3 % carbon and 7.7 % hydrogen. The combustion of acetylene in oxygen produces a higher temperature than hydrocarbon gases [2].

Some important considerations related to the risk of using acetylene are that it is flammable and produces explosive mixtures in the air at various concentrations (2.3 – 82 %). In addition, acetylene is chemically unstable under pressure, even without air.

Table 1. Characteristics of acetylene compared to other gases [2]

Gas	Density (kg/m^3)	Calor Value (MJ/kg)	Flame Temperature (°C)	Combustion Speed (m/s)
Acetylene	1.07	48.2	3,100	13.1
Propane	2.00	46.4	2,825	3.7
Hydrogen	0.08	120	2,525	8.9

Under certain conditions, it can decompose explosively into its constituents (carbon and hydrogen). For the gas to be safely stored, the bottle is filled with a porous mass saturated with acetone which absorbs the gas when filled. The pressure inside the bottle is 2 MPa, but explosive decomposition can occur in the pipe or hose coming out of the bottle if the inside pressure exceeds 1.5 MPa [2].

In the welding industry, hydrogen has long been used as a welding and cutting fuel. Sources of hydrogen gas are obtained from various processes, including the decomposition of formic acid [3], the decomposition of ammonia [4], the electrolysis of water [5], and also the extraction of chemical and petrochemical products.

The formation of hydrogen from the electrolysis of water is currently being studied. Water is formed from two elements, namely two hydrogen atoms and one oxygen atom. Compounds of water, when separated into their constituent elements, are not gaseous but liquid (at room temperature). This could be due to oxygen being more electronegative than hydrogen [6]. These properties can be used to decompose water into its constituent elements (hydrogen and oxygen) by the electrolysis method. The result of the electrolysis of water produces hydrogen and oxygen gas or hydrogen oxide hydrogen gas (HHO), also known as Brown gas which is taken from the name of its inventor, Yull Brown [7]. The electrolysis reaction of water can be seen in Figure 1.

Hydrogen is used as an alternative fuel because it has unique characteristics. As a renewable energy source, it is environmentally friendly with no emissions. In addition, hydrogen is non-toxic, colorless and undergoes a complete combustion reaction [8]. When hydrogen burns, what is produced is water. Therefore, the development of hydrogen as a fuel source will be studied and used as an alternative to acetylene in the welding process.

A dry cell HHO generator is a generator with electrodes not immersed in an electrolyte solution. In this type of generator, the electrolyte fills the gaps between the lined electrodes so that the electrolysis process occurs when the electrolyte flows through the electrodes. The electrolyte solution is accommodated in a reservoir that is stored above the electrolyzer [11][12].

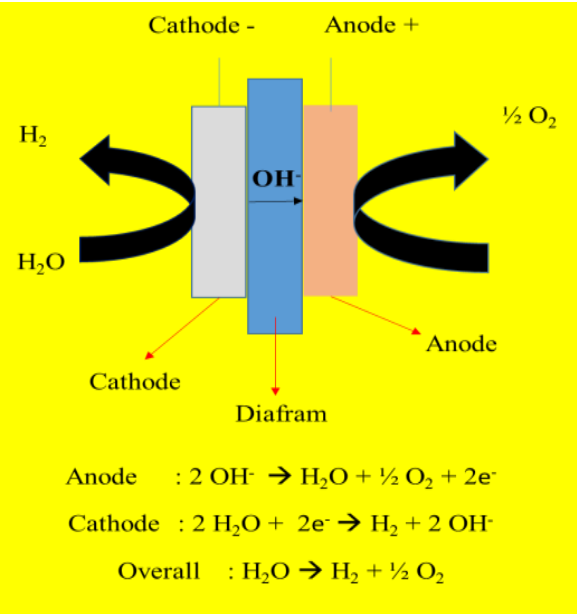

Figure 1. Electrolysis reaction of water

Based on the amount of HHO required and the available power source, the number of cells can be determined so that the effective electrode plate area can also be calculated. The number of cells and the concentration of electrolytes directly influence cell voltage. The cell voltage can be calculated by dividing the source voltages by the number of cells. Based on the previous research, the voltage required for the HHO generator to work without heating is 2-3 V [13].

The distance between the plates and the cell's operating temperature must be considered when determining the cell amperage. Since distilled water has a high resistance, an electrolyte is needed to lower it. Electrolyte concentration is highly affected by cell amperage. The current will increase during operation, which is caused by an increase in concentration due to a rise in temperature [14].

The amount of HHO depends on the efficiency of the water to transmit the electric current and the amount of current transmitted through the plate's surface. Therefore, Faraday calculated that each square inch of the plate would deliver 0.54 A.

While the amount of HHO gas production can be estimated based on (1) Faraday's law as follows [15]:

$$V = \frac{RITt}{zFP} \quad (1)$$

V is the volume of HHO gas produced in liters (L). *R* is the ideal gas constant of 0.820 atm/(mol.K). *I* is the current supplied to the generator in amperes (A). *T* is the electrolyte temperature in Calvin (K). *t* is the operating time in seconds (s). *z* is the number of electrons, i.e. two hydrogen electrons andfour4 oxygen electrons. *F* is Faraday's constant 96,485 C/mol. *P* is the pressure in units of the atmosphere (atm).

The efficiency of the HHO generator [16] can be calculated by (2).

$$\text{HHO generator efficiency} = \frac{m_{HHO} * LHV_{HHO}}{\text{Volt} * \text{Ampere} * \text{Time}} \quad (2)$$

m_{HHO} is an electrolyte concentration. LHV_{HHO} is a constant calorific value (121,000 kJ/kg).

Previous studies explained that several parameters could affect the performance of the HHO generator, including configuration and number of electrode plates [17][18], electrode distance [19][20], type of catalyst [21], electrolyte concentration [22], and current control [23-25]. Thus, we chose these five parameters as the experimental design.

Taguchi's method defines optimal process parameters and pays equal attention to yield, productivity, capacity, and cost. The application of the Taguchi method is to optimize the amount of HHO gas produced and generator efficiency. Other studies [26][27] on HHO-based welding only describe assembly without paying attention to the study of existing parameters as well as its method simulation. This study aims to study the proper parameters for the assembly of the HHO-based welding system. In this study, the combination of various potential parameters with more levels so that the calculations and results obtained by the Taguchi method will be applied as the main reference for the empirical design of the experimental and prototyping of the HHO-based welding machine.

METHOD

Experimental Design

The general concept of DOE involves the investigation of all combinations (full factorial) or exclusively restricted to a portion of the possible combinations (fractional factorial) of factors that are mostly overlooked by the trial-and-error method. However, when the process is affected by several parameters, full factorial is very costly and labor-intensive; and a fractional factorial, which increased the number of experiments to a practically satisfactory level, is too complicated, and there are no general procedures to analyze the results obtained by performing the experiments. In this case, Taguchi's proposed method is more appropriate. Taguchi method is a simpler, economical, quicker, and more feasible method for designing high-quality processes with less dispersion for experiments and recognizing proper factors for control to achieve the optimum results. Taguchi utilizes a special orthogonal array (OA), signal-to-noise (S/N) ratios, main effects, and analysis of variance (ANOVA) [9].

OA is used to study the whole process with a much-reduced number of experiments. S/N performs objective functions for optimization, which can be of three types as a rule, “smaller is better,” “larger is better,” and “nominal is the best.” In addition, they measure the degree of deviation from the desired quality characteristics.

According to the Taguchi method, robust design and an L’16 (54) OA are employed for experimentation in the present study. The signal-to-noise (S/N) ratio is the standard mean deviation ratio that performs the objective functions for the optimization process.

In interpreting the variety of factors in the process, Taguchi classifies the Signal-to-Noise Ratio (S/N Ratio) into three types, namely [26] as presented in the (3), (4), and (5):

1. Smaller The Better (STB)

$$\frac{S}{N} = -10\,LOG\left(\frac{1}{n}\sum_{k=1}^{n} yi^2\right) \quad (3)$$

2. Larger The Better (LTB)

$$\frac{S}{N} = -10\,LOG\left(\frac{1}{n}\sum_{k=1}^{n} \frac{1}{yi^2}\right) \quad (4)$$

3. Nominal The Better (NTB)

$$\frac{S}{N} = -10\,LOG\left(\frac{1}{n}\sum_{k=1}^{n} \frac{\sigma^2}{yi^2}\right) \quad (5)$$

Preparation and Measurement

Figure 2 shows the schematic of the developed HHO-based welding, including its instrumentation system. The E-9 is a power supply of a 12 V battery for the HHO G-1 generator. The power supply is connected in series with a standard resistance I-12, to which a voltmeter I-13 is connected to measure current density. Finally, the I-14 voltmeter is installed in parallel to measure the electrode voltage, representing the HHO generator's efficiency.

E-2 is a feed water tank that contains an electrolyte solution for the HHO P-3 generator, which is channelled automatically by the E-4 pump with ON-OFF command from the I-2 level indicator. When the I-2 level shows a Low Level, then the E-4 pump drive motor will turn ON. After the level shows a High Level then, the E-4 pump drive motor will turn OFF.

The electrolyzed gas is separated between oxygen and hydrogen. Oxygen will go to the E-7 tube through the E-5 bubbler with a V-1 check valve installed to anticipate the pressure backflow. Meanwhile, hydrogen will flow to the E-6 bubbler, which has a V-2 check valve installed. In each hydrogen and oxygen line, flow rate measuring devices are installed in the form of rotameters I-8 and I-7. In addition, each gas storage tube is installed with a Pressure Safety Valve (PSV) V-3 and V-4, which will open in case of overpressure.

A pressure indicator is installed on each storage tube which is also connected to the PLC I-10, which will turn off the system if overpressure exceeds the design limit or the PSV fails to work. E-1 is a cooling fan that will turn on in case overheating happens.

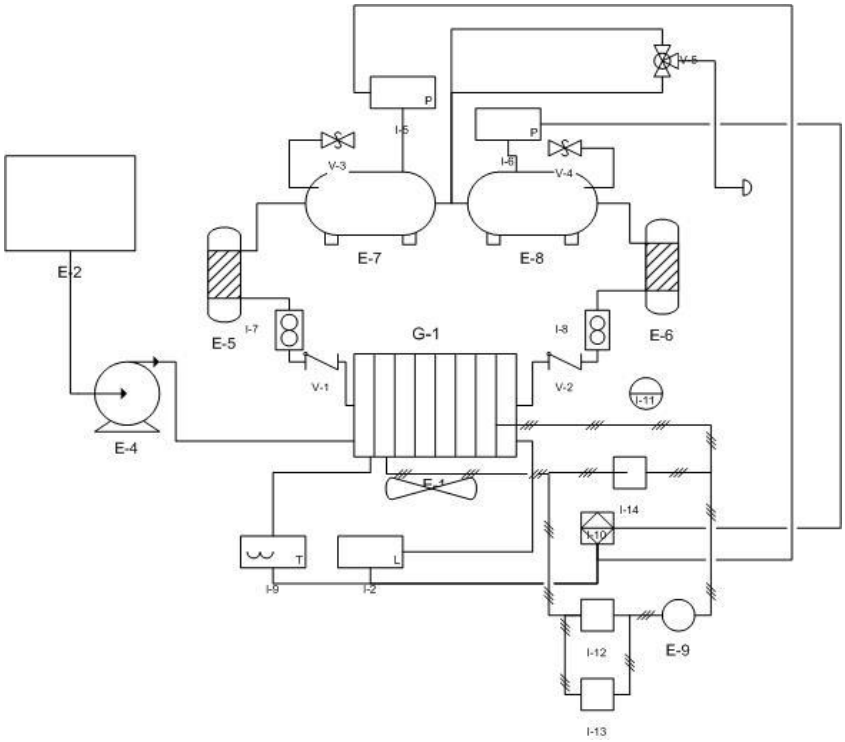

Figure 2. Schematic of HHO-based welding system.

In this study, the materials used are as follows:

Electrode Plate

The assembled HHO generator, as seen in Figure 3, consists of a titanium plate as the cathode and a platinum-coated titanium plate as the anode. Those plates are the used material from the sodium hypochlorite generator of Badak LNG Bontang.

Gasket

Gaskets are used as a separator between rubber-based plates. The gasket must be insulating so that each electrode plate is not connected to the others (avoid the shortcut).

Acrylic

Acrylic is used as the cover body of the reactor, acrylic was chosen due to its easiness of fabrication, good heat resistance, high-pressure resistant, and transparency, so it is easy to observe the system.

Cylinder Bomb

The cylinder bomb with a pressure specification of 6 barg is used to accommodate the electrolysis gases.

The catalyst materials used in this work are potassium hydroxide (KOH), sodium hydroxide (NaOH), and sodium bicarbonate ($NaHCO_3$).

In addition, the plate configuration is also varied, with the number of neutral plates, anodes and cathodes. The PWM duty cycle variation determines the current's effect on generator performance. The thickness of the gasket is also varied in this study to determine the significance of the distance between the plates. Table 2 shows the variation of parameters carried out in this work. Table 3 is an experimental design based on the orthogonal array of the Taguchi experiment.

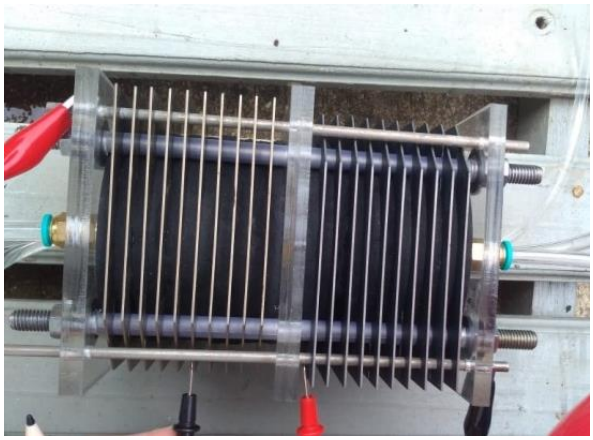

Figure 3. Photograph of HHO Generator

Table 2. Design of experiments with five factors and four levels

	Factor	Level 1	Level 2	Level 3	Level 4
A	Plate configuration	3A3C15N	4A4C14N	5A5C9N	10A10C0N
B	Catalyst	NaOH	KOH	NaHCO3	Non Catalyst
C	Electrolyte concentration (M)	0.10	0.15	0.20	0.25
D	PWM Duty Cycle (%)	40	60	80	100
E	Gasket Thickness (mm)	2.4	3.2	4.0	4.8

Table 3. Taguchi's design experiments

Run	A	B	C (M)	D (%)	E (mm)
1	3A3C15N	NaOH	0.1	40	2.4
2	3A3C15N	KOH	0.15	60	3.2
3	3A3C15N	$NaHCO_3$	0.2	80	4.0
4	3A3C15N	Non Catalyst	0.25	100	4.8
5	4A4C14N	NaOH	0.15	80	4.8
6	4A4C14N	KOH	0.1	100	4.0
7	4A4C14N	$NaHCO_3$	0.25	40	3.2
8	4A4C14N	Non Catalyst	0.2	60	2.4
9	5A5C9N	NaOH	0.2	100	3.2
10	5A5C9N	KOH	0.25	80	2.4
11	5A5C9N	$NaHCO_3$	0.1	60	4.8
12	5A5C9N	Non Catalyst	0.15	40	4.0
13	10A10C0N	NaOH	0.25	60	4.0
14	10A10C0N	KOH	0.2	40	4.8
15	10A10C0N	$NaHCO_3$	0.15	100	2.4
16	10A10C0N	Non Catalyst	0.1	80	3.2

The data taken from the research are the amount of HHO gas production per unit of time, the current consumed by the generator as a representation of efficiency, the delta temperature of electrolyte and the welding temperature of the HHO gas.

RESULTS AND DISCUSSION

Welding System and Flame

All components on the welding system, including the HHO storage cylinder, have gone through a pneumatic test to a targeted pressure of 3.5 bar to confirm its maximum safety for operation. The testing process is shown in Figures 4 and 5. The HHO-based welding system that has completed the fabrication process is shown in Figure 6, and the photograph of the welding flame torch is shown in Figure 7.

Figure 4. Pneumatic test setup for HHO gas storage cylinder

Figure 5. Pneumatic test readings for HHO gas storage cylinder

Figure 6. Prototype of HHO-based welding system

Figure 7. Photograph of HHO based welding flame from a welding torch

Level Factor Analysis on Current Consumption

The experimental data that has been obtained from measuring the current consumption of the HHO generator on the welding equipment are presented in Table 4. The S/N ratio used in the current consumption calculation is Smaller The Better (STB), so a graph plot is obtained, as shown in Figure 8. In Table 5, it can be seen that the variable that has the most influence on decreasing the current consumption of the HHO generator is variable A (plate configuration). At the same time, the percentage contribution of each factor is shown in Table 6, where the plate configuration has the largest contribution of 57.68 %. Current consumption increases by 51 % when plate configuration is changed from 3A3C15N to 4A4C14N, increases by 56 % when changed from 4A4C14N to 5A5C9N, and increase by 47 % when changed from 5A5C9N to 10A10C0N. The most optimal result for current consumption is in the 3rd type of experiment, with 3A3C15N, $NaHCO_3$, 0.2 M electrolyte concentration, 80 % PWM, and 4.0 mm gasket distance.

Table 4. The results of measuring current consumption on the HHO generator

Run	A	B	C (M)	D (%)	E (mm)	Mean (A)	S/N
1	3A3C15N	NaOH	0.1	40	2.4	2.50	-7.95
2	3A3C15N	KOH	0.15	60	3.2	5.32	-14.52
3	3A3C15N	$NaHCO_3$	0.2	80	4.0	1.32	-2.42
4	3A3C15N	Non Catalyst	0.25	100	4.8	3.89	-11.8
5	4A4C14N	NaOH	0.15	80	4.8	7.76	-17.8
6	4A4C14N	KOH	0.1	100	4.0	12.42	-21.9
7	4A4C14N	$NaHCO_3$	0.25	40	3.2	4.05	-12.14
8	4A4C14N	Non Catalyst	0.2	60	2.4	2.53	-8.07
9	5A5C9N	NaOH	0.2	100	3.2	30.79	-29.77
10	5A5C9N	KOH	0.25	80	2.4	23.87	-27.56
11	5A5C9N	$NaHCO_3$	0.1	60	4.8	4.25	-12.58
12	5A5C9N	Non Catalyst	0.15	40	4.0	2.08	-6.38
13	10A10C0N	NaOH	0.25	60	4.0	38.50	-31.71
14	10A10C0N	KOH	0.2	40	4.8	28.77	-29.18
15	10A10C0N	$NaHCO_3$	0.15	100	2.4	36.88	-31.34
16	10A10C0N	Non Catalyst	0.1	80	3.2	11.26	-21.04

Table 5. S/N ratio response to current consumption

Level	A	B	C	D	E
1	-9.17	-21.81	-15.87	-13.91	-18.73
2	-14.98	-23.29	-17.51	-16.72	-19.37
3	-19.07	-14.62	-17.36	-17.2	-15.6
4	-28.32	-11.82	-20.8	-23.7	-17.84
Delta	19.15	11.46	4.94	9.79	3.77
Rank	1	2	4	3	5

Table 6. Analysis of Variance (ANOVA) for current consumption levels

Source	DF	Adj SS	Contribution (%)	Adj MS	F-Value	P-Value
A	3	1560.15	57.68	520.05	*	*
B	3	537.43	19.87	179.14	*	*
C	3	228.49	8.44	76.16	*	*
D	3	320.44	11.85	106.81	*	*
E	3	58.14	2.15	19.38	*	*
Error	0	*		*		
Total	15	2704.65	100			

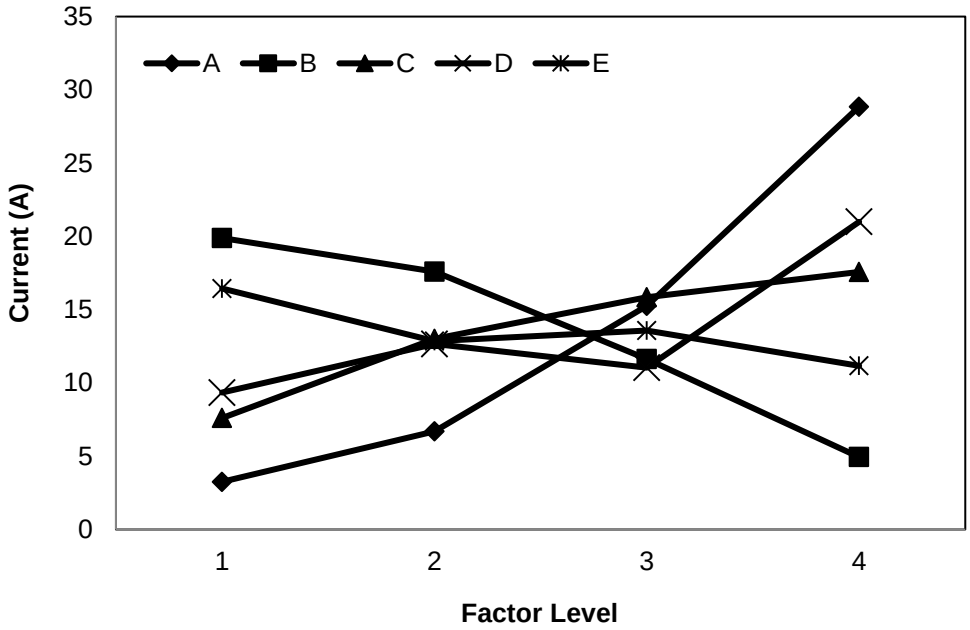

Figure 8. The plot of the mean response of current consumption

Level Factor Analysis on Electrolyte Temperature

The experimental data obtained from measuring the temperature rise of the electrolyte in the welding equipment are shown in Table 7. The Smaller The Better (STB) mode is the S/N ratio used in calculating the temperature increase is the Smaller The Better (STB) mode. Its graph plot is presented in Figure 9. Meanwhile, Table 8 shows that the most influential variable on the increase in electrolyte temperature is Variable C (electrolyte concentration).

The percentage contribution of each factor is shown in Table 9, where the electrolyte concentration has the largest contribution of 36.4 %. The temperature rise was drastically reduced by 73.8 % when the electrolyte concentration was changed from 0.1 to 0.15 M. The most optimal result for the increase in electrolyte temperature was in the 7th experiment, i.e. the 4A4C14N, $NaHCO_3$ catalyst type, electrolyte concentration 0.25 M, 40% PWM, and 3.2 mm gasket thickness.

Table 7. The results of measuring increasing the electrolyte temperature

Run	A	B	C (M)	D (%)	E (mm)	Mean (°C)	S/N
1	3A3C15N	NaOH	0.1	40	2.4	1.17	-1.39
2	3A3C15N	KOH	0.15	60	3.2	0.20	10.62
3	3A3C15N	$NaHCO_3$	0.2	80	4.0	0.10	17.78
4	3A3C15N	Non Catalyst	0.25	100	4.8	2.33	-7.39
5	4A4C14N	NaOH	0.15	80	4.8	1.27	-2.1
6	4A4C14N	KOH	0.1	100	4.0	4.17	-12.45
7	4A4C14N	$NaHCO_3$	0.25	40	3.2	0.03	24.77
8	4A4C14N	Non Catalyst	0.2	60	2.4	0.10	17.78
9	5A5C9N	NaOH	0.2	100	3.2	0.87	1.15
10	5A5C9N	KOH	0.25	80	2.4	0.50	5.28
11	5A5C9N	$NaHCO_3$	0.1	60	4.8	2.62	-8.51
12	5A5C9N	Non Catalyst	0.15	40	4.0	0.13	14.77
13	10A10C0N	NaOH	0.25	60	4.0	2.80	-9.03
14	10A10C0N	KOH	0.2	40	4.8	1.53	-3.79
15	10A10C0N	$NaHCO_3$	0.15	100	2.4	0.83	1.1
16	10A10C0N	Non Catalyst	0.1	80	3.2	1.33	-2.54

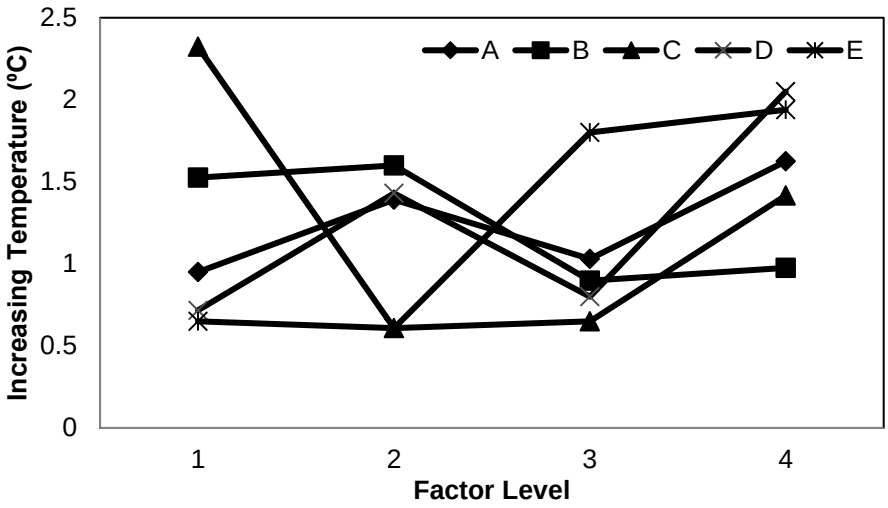

Figure 9. The plot of the mean response to increasing the electrolyte temperature

Table 8. S/N ratio response to the increasing temperature of the electrolyte

Level	A	B	C	D	E
1	4.91	-2.84	-6.22	8.6	5.7
2	7.0	-0.08	6.1	2.7	8.5
3	3.17	8.79	8.23	4.61	2.77
4	-3.57	5.66	3.41	-4.4	-5.45
Delta	10.57	8.49	14.45	12.99	13.95
Rank	4	5	1	3	2

Table 9. Analysis of Variance (ANOVA) for the increasing temperaturethe of electrolyte

Source	DF	Adj SS	Contribution (%)	Adj MS	F-Value	P-Value
A	3	1.195	5.58	0.3983	*	*
	3	1.592	7.43	0.5307	*	*
C	3	7.799	36.4	2.5997	*	*
D	3	4.639	21.65	1.5462	*	*
E	3	6.197	28.93	2.0656	*	*
Error	0	*		*		
Total	15	21.421	100			

Level Factor Analysis of HHO Flow Rate

The experimental data that has been obtained from the measurement of the HHO flow rate produced by the generator on the welding tool is in Table 10. The S/N ratio used in calculating the HHO gas flow rate is The Larger The Better (LTB) mode and its graph plot is presented in Figure 10. It can be seen that variable B (catalyst type) has the most positive effect on the increase in flow rate. At the same time, the percentage contribution of each factor is shown in Tables 11 and 12, where the type of catalyst has the largest contribution of 36.4 %. The HHO flow rate increased by 7 % when the catalyst changed from NaOH to KOH, decreased by 52 % when the catalyst became $NaHCO_3$ and decreased by 51 % when the catalyst changed from $NaHCO_3$ to without a catalyst.

The most optimal results for the HHO flow rate were in the 9th experiment, i.e., the 5A5C9N, the type of catalyst was NaOH, the electrolyte concentration was 0.2 M, PWM 100 %, and the gasket thickness was 3.2 mm.

Level Factor Analysis on the efficiency of the HHO generator

The experimental data obtained from the generator's efficiency measurements on the welding equipment are listed in Table 13. The S/N ratio used in the generator efficiency calculation is the Larger The Better (LTB), and its graph plot is shown in Figure 11. Table 14 shows that variable A (plate configuration) has the most positive effect on increasing efficiency.

In contrast, the percentage contribution of each factor is shown in Table 15, where the plate configuration has the largest contribution, i.e., 57.73 %.

Table 10. The results of measuring HHO flowrate

Run	A	B	C (M)	D (%)	E (mm)	Mean (ml/second)	S/N
1	3A3C15N	NaOH	0.1	40	2.4	51.97	34.31
2	3A3C15N	KOH	0.15	60	3.2	149.53	43.49
3	3A3C15N	$NaHCO_3$	0.2	80	4.0	33.22	30.42
4	3A3C15N	Non Catalyst	0.25	100	4.8	115.54	41.25
5	4A4C14N	NaOH	0.15	80	4.8	149.39	43.49
6	4A4C14N	KOH	0.1	100	4.0	308.98	49.76
7	4A4C14N	$NaHCO_3$	0.25	40	3.2	53.25	34.53
8	4A4C14N	Non Catalyst	0.2	60	2.4	31.36	29.93
9	5A5C9N	NaOH	0.2	100	3.2	527.60	54.44
10	5A5C9N	KOH	0.25	80	2.4	445.94	52.97
11	5A5C9N	$NaHCO_3$	0.1	60	4.8	69.40	36.83
12	5A5C9N	Non Catalyst	0.15	40	4.0	22.07	26.88
13	10A10C0N	NaOH	0.25	60	4.0	394.58	51.92
14	10A10C0N	KOH	0.2	40	4.8	299.73	49.53
15	10A10C0N	$NaHCO_3$	0.15	100	2.4	416.95	52.38
16	10A10C0N	Non Catalyst	0.1	80	3.2	108.19	40.67

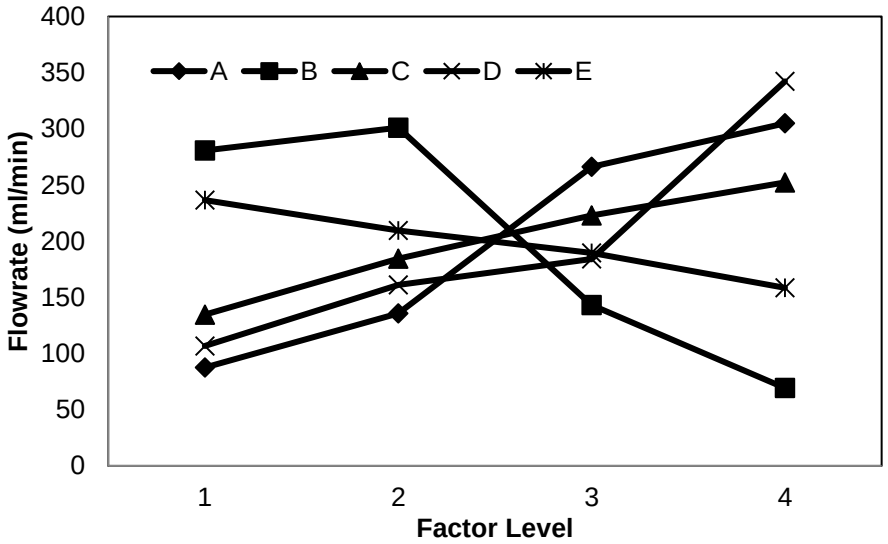

Figure 10. The plot of the mean response of HHO flowrate

Table 11. S/N ratio response to HHO flowrate

Level	A	B	C	D	E
1	37.37	46.04	40.39	36.31	42.4
2	39.42	48.94	41.56	40.54	43.28
3	42.78	38.54	41.08	41.89	39.74
4	48.63	34.68	45.17	49.46	42.77
Delta	11.26	14.26	4.77	13.15	3.54
Rank	3	1	4	2	5

Table 12. Analysis of Variance (ANOVA) for HHO flowrate

Source	DF	Adj SS	Contribution (%)	Adj MS	F-Value	P-Value
A	3	128,59	28.98	42,86	*	*
B	3	148,22	33.41	49,41	*	*
C	3	31,085	7	10,36	*	*
D	3	122,72	27.66	40,91	*	*
E	3	12,99	2.93	4,33	*	*
Error	0	*		*		
Total	15	443,62	100			

Table 13. The results of measuring the efficiency of the HHO generator

Run	A	B	C (M)	D (%)	E (mm)	Mean (%)	S/N
1	3A3C15N	NaOH	0.1	40	2.4	23	-9.31
2	3A3C15N	KOH	0.15	60	3.2	46	-6.65
3	3A3C15N	$NaHCO_3$	0.2	80	4.0	42	-7.59
4	3A3C15N	Non Catalyst	0.25	100	4.8	49	-6.19
5	4A4C14N	NaOH	0.15	80	4.8	32	-9.94
6	4A4C14N	KOH	0.1	100	4.0	41	-7.72
7	4A4C14N	$NaHCO_3$	0.25	40	3.2	22	-13.24
8	4A4C14N	Non Catalyst	0.2	60	2.4	21	-13.76
9	5A5C9N	NaOH	0.2	100	3.2	28	-10.95
10	5A5C9N	KOH	0.25	80	2.4	31	-10.2
11	5A5C9N	$NaHCO_3$	0.1	60	4.8	27	-11.38
12	5A5C9N	Non Catalyst	0.15	40	4.0	18	-15.13
13	10A10C0N	NaOH	0.25	60	4.0	17	-15.42
14	10A10C0N	KOH	0.2	40	4.8	17	-15.27
15	10A10C0N	$NaHCO_3$	0.15	100	2.4	19	-14.56
16	10A10C0N	Non Catalyst	0.1	80	3.2	16	-15.97

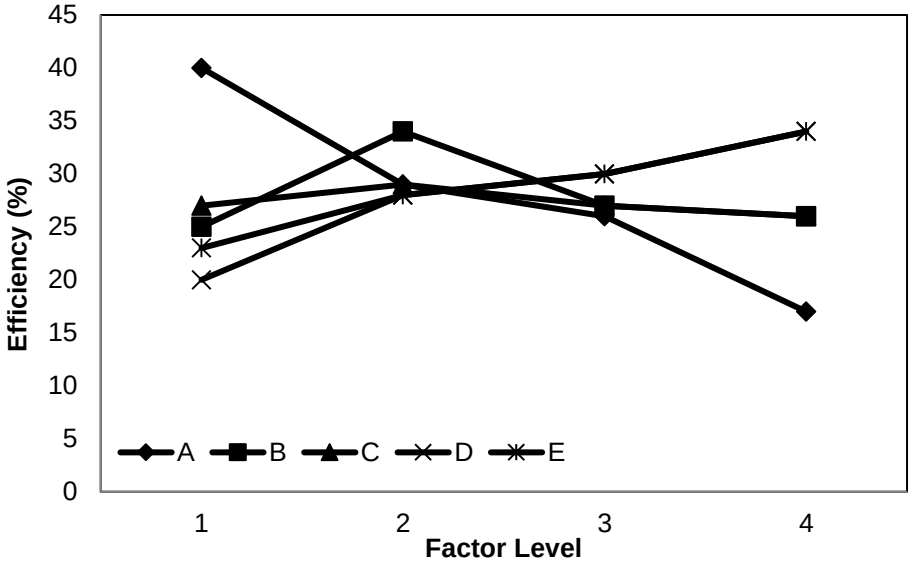

Figure 11. The plot of the mean response of efficiency of the HHO generator

Table 14. S/N ratio response to the efficiency of the HHO generator

Level	A	B	C	D	E
1	-7.44	-11.41	-11.09	-13.24	-11.96
2	-11.17	-9.96	-11.57	-11.80	-11.70
3	-11.92	-11.69	-11.9	-10.93	-11.47
4	-15.31	-12.76	-11.26	-9.85	-10.7
Delta	7.87	2.8	0.8	3.39	1.27
Rank	1	3	5	2	4

Table 15. Analysis of Variance (ANOVA) for efficiency of HHO generator

Source	DF	Adj SS	Contribution (%)	Adj MS	F-Value	P-Value
A	3	1,058.19	57.73	352.729	*	*
B	3	185.19	10.1	61.729	*	*
C	3	24.69	1.35	8.229	*	*
D	3	432.69	23.6	144.229	*	*
E	3	132.19	7.2	44.063	*	*
Error	0	*		*		
Total	15	1832.94	100			

Figure 12. Flame temperature measurement

Table 16. Flame temperature of HHO welding

Experiment Number	Maximum Temperature (°C)
1	1,020.6
2	1,080.8
3	1,070.9
4	1,083.1

The efficiency was reduced by 28 % when the plate configuration was changed from 3A3C15N to 4A4C14N, decreased by 9.9 % when the plate configuration was changed from 4A4C14N to 5A5C9N and again reduced by 33 % when the plate configuration was changed from 5A5C9N to 10A10C0N. The most optimal result for efficiency was in the 4th experiment, i.e., the 3A3C15N, without catalyst, 100 % PWM, and 4.8 mm gasket thickness.

Combustion Temperature

Combustion Temperature HHO gas that has been accommodated in the tube, then the combustion temperature data is taken by a thermocouple as shown in Figure 12. The results are listed in Table 16.

CONCLUSION

The HHO gas-based welding equipment design consists of various basic components: a dry cell generator made of titanium as a cathode plate and platinum-coated titanium as an anode, a bubbler, a gas storage tank, a box with a cooling fan, and a welding torch. From the Taguchi calculations, the optimal design for a dry cell generator is obtained, namely the configuration of three anodes, three cathodes and 15 neutral plates (3A3C15N), KOH catalyst type, electrolyte concentration 0.15 M, PWM duty cycle 60%, and gasket spacing between plates 3.2 mm. The design has an average current consumption of 5.32 A, a temperature increase of 0.2 °C, an HHO gas flow rate of 149,53 mL/minute, and an efficiency of 46%. Plate configuration is the variable that has the most influence on decreasing current consumption and increasing the efficiency of the HHO generator. At the same time, the electrolyte concentration variable has the most effect on suppressing the temperature rise. Finally, the variable type of catalyst has the most positive effect on increasing the flow rate of HHO. Thus, the resulting HHO gas is burned through a welding torch, and the average value of the combustion temperature is about 1,063.85 °C.

ACKNOWLEDGMENT

This research was supported by Badak LNG and LNG Academy, East Borneo.

REFERENCES

[1] S. Sukarman et al., “Optimization of the resistance spot welding process of secc-af and sgcc galvanized steel sheet using the Taguchi Method,” *SINERGI*, vol. 25, no. 3, pp. 319-328, 2021, doi: 10.22441/sinergi. 2021.3.009

[2] R. S. Rachmat, “Analysis of Welding Procedure Specifications for steel line pipe material,” *SINERGI*, vol. 26, no. 3, pp. 279-286, 2022, doi: 10.22441/sinergi.2022.3.002

[3] S. Patra and S. K. Singh, “Hydrogen Production from Formic Acid and Formaldehyde over Ruthenium Catalysts in Water,” *Inorg. Chem.*, vol. 59, no. 7, pp. 4234–4243, 2020, doi: 10.1021/acs. inorgchem.9b02882.

[4] D. K. Lim *et al.*, “Solid Acid Electrochemical Cell for the Production of Hydrogen from Ammonia,” *Joule*, vol. 4, no. 11, pp. 2338–2347, 2020, doi: 10.1016/j.joule. 2020.10.006.

[5] Rusdianasari et al., “HHO Gas Generation in Hydrogen Generator using Electrolysis,” *IOP Conference Series: Earth and Environmental Science*, vol. 258, no. 1. 2019, doi: 10.1088/1755-1315/258/1/012007.

[6] S. Pamfrord et al., “Design and Development of an Oxyhydrogen Generator for Production of Brown’s (HHO) Gas as a Renewable Source of Fuel for the Automobile Industry”, *International Journal of Engineering Science Invention (IJESI),* vol. 8, no. 05, pp. 01-07, 2019,

[7] T. B. Arjun et al., “A review on analysis of HHO gas in IC engines,” *Mater. Today Proc.*, vol. 11, pp. 1117–1129, Jan. 2019, doi: 10.1016/j.matpr.2018.12.046.

[8] B. Subramanian, “Experimental investigations on performance, emission and combustion characteristics of Diesel-Hydrogen and Diesel-HHO gas in a Dual fuel CI engine”, *International Journal of Hydrogen Energy*, vol 45, 2020, doi: 10.1016/j.ijhydene.

2020.06.280.
[9] A. Parnianifard, A. S. Azfanizam, M. K. A. Ariffin, and M. I. S. Ismail, "Robust Product Design : A Modern View of Quality Engineering in Manufacturing Systems," *Int. J. Recent Adv. Multidiscip. Res.*, vol. 4, no. 12, pp. 3220–3225, 2017.
[10] I. Elgarhi, "Enhancing compression ignition engine performance using biodiesel/diesel blends and HHO gas", *International Journal of Hydrogen Energy*, vol 45, 2020, doi: 10.1016/j.ijhydene.2020.06.273.
[11] P. Jaklinski, "An experimental investigation of the impact of added HHO gas on automotive emissions under idle conditions," *Int. J. Hydrogen Energy*, vol. 45, no. 23, pp. 13119–13128, 2020, doi: 10.1016/j.ijhydene. 2020.02.225.
[12] S. M. Pourkiaei et al., "Thermoelectric cooler and thermoelectric generator devices: A review of present and potential applications, modeling and materials," *Energy*, vol. 186, 2019, doi: 10.1016/j.energy.2019.07.179
[13] B. Boyce, "Additives that Improve Mileage," 2016.
[14] T. Nabil and M. M. Khairat Dawood, "Enabling efficient use of oxy-hydrogen gas (HHO) in selected engineering applications; transportation and sustainable power generation," *J. Clean. Prod.*, vol. 237, p. 117798, 2019, doi: 10.1016/j.jclepro. 2019.117798.
[15] L. Bella, "HHO Dry Cell Kits & Accessories," 2003. https://labellashho.com/fueledbywater.htm (accessed Oct. 25, 2020).
[16] M. El-Kassaby, "Effect of hydroxy (HHO) gas addition on gasoline engine performance and emiss ions," *Alexandria Eng. J.*, vol. 55, no. 1, pp. 243–251, 2016, doi: 10.1016/ j.aej.2015.10.016.
[17] M. A. El Kady, "Parametric study and experimental investigation of hydroxy (HHO) production using dry cell," *Fuel*, vol. 282, 2020, doi: 10.1016/j.fuel.2020.118825.
[18] T. Nabil, "Enabling efficient use of oxy-hydrogen gas (HHO) in selected engineering applications; transportation and sustainable power generation," *J. Clean. Prod*., vol. 237, 2019, doi: 10.1016/j.jclepro.2019.117798.
[19] M. Kady, "Parametric study and experimental investigation of hydroxy (HHO) production using dry cell," *Fuel*, vol 282, 2020, doi: 10.1016/j.fuel.2020.118825.
[20] A. Al-Rousan, "Effect of anodes-cathodes inter-distances of HHO fuel cell on gasoline engine performance operating by a blend of HHO," *Int. J. Hydrogen Energy*, vol. 43, no. 41, pp. 19213–19221, 2018, doi: 10.1016/j.ijhydene.2018.08.118.
[21] H. Prasetya, "The experimental study of wet cell HHO generator type with Ba $(OH)_2$ catalyst on performance and exhaust gaseous emissions of 4 stroke engine 120 cc," *AIP Conference Proceedings*, vol. 1977. 2018, doi: 10.1063/1.5043026.
[22] N. Alam, "Experimental Study of Hydroxy Gas (HHO) Production with Variation in Current, Voltage and Electrolyte Concentration", *IOP Conference Series: Materials Science and Engineering*, vol 225, 2017, doi: 10.1088/1757-899X/225/1/ 012197.
[23] Ç. Conker, "A novel fuzzy logic based safe operation oriented control technique for driving HHO dry cell systems based on PWM duty cycle," *Int. J. Hydrogen Energy*, vol. 44, no. 20, pp. 9718–9725, 2019, doi: 10.1016/j.ijhydene.2018.10.243.
[24] Bambang. S., "Application of Dry Cell Hho Gas Generator With Pulse Width Modulation on Sinjai Spark Ignition Engine Performance," *Int. J. Res. Eng. Technol*., vol. 05, no. 02, pp. 105–112, 2016, doi: 10.15623/ijret.2016.0502019.
[25] N. Alam, "Experimental Study of Hydroxy Gas (HHO) Production with Variation in Current, Voltage and Electrolyte Concentration," *IOP Conference Series: Materials Science and Engineering*, vol. 225, no. 1. 2017, doi: 10.1088/1757-899X/225/1/ 012197.
[26] R. Kesarwani, M. Ariz, N. Kumar, "HHO Generation & Its Application on Welding HHO Generation & Its Application on Welding", *IJSRD - International Journal for Scientific Research & Development,* vol. 5, no. 09, 2017
[27] R. Kesarwani, M. Ariz, and N. Kumar, "HHO Generation & Its Application on Welding HHO Generation & Its Application on Welding," *IJSRD - Int. J. Sci. Res. Dev*., vol. 5, no. 09, pp. 579–582, 2017.
[28] P. P. Kumar, "Development and applications of HHO water based flame torch," *Int. J. Recent Technol. Eng*., vol. 7, no. 6, pp. 515–517, 2019.
[29] Musabbikhah et al., "Modelling and optimization of the best parameters of rice husk drying and carbonization by using Taguchi method with multi response signal to noise procedure," *Int. J. Renew. Energy Res.*, vol. 7, no. 3, pp. 1219–1227, 2017.